ABUAD Journal of Engineering Research and Development (AJERD)
ISSN (online): 2645-2685; ISSN (print): 2756-6811

Volume 5, Issue 1, 93-109

Extraction of Nano-Chitosan from Waste White Shrimp Shells for Removal of Phenol from Refinery Wastewater: Optimization of Chitosan Synthesis and Phenol Adsorption

Abubakar Abubakar IBRAHIM[1], Abdulfatai JIMOH[1], Yahya Muibat DIEKOLA[2], Manase AUTA[2]

[1]*Department of Chemical Engineering, Faculty of Engineering, University of Abuja, P.M.B.117, Abuja, Nigeria*
abubakar6989@gmail.com/ fatai2011@yahoo.com

[2]*Department of Chemical Engineering, School of Infrastructure, Process Engineering and Technology, Federal University of Technology Minna; P.M.B. 65, Minna, Niger State, Nigeria*
muibat.yahya@futminna.edu.ng/ manaseauta@yahoo.com

Corresponding Author: abubakar6989@gmail.com, +2348032670719

Date Submitted: 05/02/2022
Date Accepted: 02/06/2022
Date Published: 30/06/2022

Abstract: *The waste generated from production and processing of aquatic and petroleum resources constitute major source of pollution in our environment. However, this research work aims at optimization of both phenol adsorption and low molecular weight nano – chitosan synthesis from waste white shrimp shells. The optimization of nano – chitosan from waste white shrimp shells was carried out. Design of experiment (DOE) technique was considered to prepared an experimental matrix using central composite design (CCD) approach. Response surface methodology (RSM) was applied to optimize the process parameters to achieved model validated degree of demineralization, deproteination, deacetylation of chitin and nano-chitosan size efficiency. Results revealed degree of demineralization, deproteination of chitin and deacetylation of chitosan were 99.57%, 96.4% and 91.20% respectively. The molecular weight of chitosan was 21374 Da, which indicates that the chitosan obtained was low molecular weight and has the potential for various technological usage. Analysis of the synthesized nano–chitosan displays a size of 84.36 nm through Dynamic Light Scattering (DLS) with more surface areas for phenol removal and adsorption processes. Fourier transform infrared spectrometer (FT-IR) and High-resolution Scanning electron microscopy (SEM) was used for characterization. The concentrations of refinery wastewater before and after treatment was carried out with aid of Double beam UV – spectrophotometer and obtained values was 7.18 and 0.033 mg/l respectively. The removal efficiency of phenol was obtained from RSM and model validation values for both experimental and predicted values of 97.22 % and 97.61% respectively, at factors of 3.86 g, 59.20 ^{o}C and 98 mins. The obtained results agreement with the statistical model, confirming that RSM can be used effectively to optimize process parameters.*

Keywords: *Phenol, Waste white shrimp shells, deacetyl chitin, nano-chitosan, refinery wastewater.*

1. INTRODUCTION

Phenol and its compounds are among the most common organic pollutants that are present in untreated or not properly treated wastewater from petroleum, plastic, pesticides, pharmaceutical and steel industries [1, 2]. The concentration of phenol in some of the wastewater varies from 0.1 - 6,800 mg/l (21.15 mg/l was found in the wastewater under investigation) as against permissible limit of 0.5 mg/l (Federal Environmental Protection Agency, FEPA) [3, 4] and maximum amount of 0.001 mg/l in portable water (FEPA and World Health Organization, WHO) [4, 5]. Phenol is considered to be a very toxic pollutant in refinery wastewater because even at low level with long exposure, it can cause severe health hazards that may include liver damage, dark urine and mouth ulcer [5]. It has been reported that due to toxic and inhibitory characteristics, phenols are very difficult to remove by biological processes [1, 3].

According to [6], various technologies such as coagulation/flocculation [4], membrane filtration [5], chemical precipitation [7] oxidation and ion exchange process [8], reverse-osmosis, electrodialysis [9], have been developed over the years for the removal of some of these contaminants from refinery and industrial wastewaters, these older technologies are found to be expensive, complicated or unnecessarily time consuming [10]. These impediments have inspired the search for more efficient and cheaper methods [11]. Recent research findings however have revealed that adsorbents containing natural polymers such as chitin and its derivatives like nano-chitosan obtained from aquatic wastes such as waste white shrimp shell are becoming more promising in the removal of pollutants from wastewater and raw water through adsorption process; although yet to be fully exploited in developing countries like Nigeria [4, 5].

Chitin is obtained through decolourization, demineralization and deproteination processes of different waste materials such as waste white shrimp shell [12, 13]. Although, it has limited area of application because of the presence of hydrogen bond and its insoluble nature in common organic solvents [14, 15]. However, chitosan has been reported to be more useful than chitin because it possesses a greater number of chelating amino groups due to the molecular weight and percentage degree of deacetylation which can be chemically modified [16]. Modification of chitosan to obtained nano-chitosan are still being actively investigated for various application [2, 17].

It has also been reported that the smaller the size of chitosan particles, the more functional groups it possesses that will enhance adsorption process [16, 18]. Nano-chitosan particles are produced through cross-linking of chitosan [19]. This is done spontaneously by ionic interaction with negatively charged of sodium tripolyphosphate (STPP), which is environmental friending compared to glutaraldehyde [19]. This biopolymer (nano-chitosan) with the specified size range is considered a suitable material for the removal of organic pollutants like phenol [16, 17]. In adsorption process for the removal of pollutants from industrial effluents or wastewaters, particle size plays vital role [18, 10].

The several process parameters used in converting of chitin to nano chitosan plays a vital role on the yield and quality of final nano chitosan [19, 7]. However, using one process parameter (factor) at a time is considered to be time consuming and expensive but also failed to elucidated the effect of other process parameters [19]. Consequently, the need for better approaches like central composite design (CCD) of experimental design and analysis of variance (ANOVA) of response surface methodology (RSM) where other process parameters are duly considered [11,20]. The major advantages of RSM over others approaches include low cost of materials and high effectiveness [21, 22]. It can also reduce the number of experimental trials, determine the significant reaction factors, as well as to optimize the treatment conditions [22].

This research work therefore focused on optimizing each stage of conversion of chitin to nano – chitosan and the effect of some major process parameters (temperature, time and concentration of organic acid/inorganic base) on the quality and quantity of nano-chitosan synthesis from locally available aquatic wastes (waste white shrimp shells-*Penaeus notialis*), with its application for the removal of phenol from refinery wastewater using response surface methodology (RSM).

2. MATERIALS AND METHODS

2.1 Preparation and Experimental Procedures

The waste white shrimp shells (WWSS) samples were obtained from Makoko, Yaba, Lagos – Nigeria and thoroughly washed with deionized water to remove dirt and dust particles. The WWSS was oven dried at 60^{o}C for 24 h and later crushed to a 300 µm BS sieve [21, 17]. The WWSS were decolourized with acetone in the ratio 1:1 weight of solid to solvent (W/V) for 2 min and dried for 1 h at ambient temperature. The decolourized WWSS samples were bleached with 0.35 % sodium hypochloride {95 %, Analar BDH-USA} solution for 2 min at an ambient temperature using a solid to solvent ratio of 1: 5 (w/v). Subsequently, washed with distilled water, filtered and oven dried for about 5 h at 60^{o}C and kept in a desiccator for subsequent analysis [19, 23]. The wastewater sample from Refining were given specific labels to avoid misrepresentation in the course of processing, stored in clean container and refrigerated. All major chemical used were of analytical grade.

2.2 Design of Experiments

The software Design Expert (Version 7.0.1, Stat-Ease) via central composite design (CCD) was broadly used for fitting a quadratic model and it requires only a minimum number of experimental runs as given by equation (1), was generated as presented in Table 1.

The responses and the corresponding parameters were modeled and optimized using ANOVA to estimate the statistical parameters by means of RSM [21]. Also, the optimization process uses four main steps, which are, executing the statistical designed experiments, estimating mathematical model coefficients, envisaging the response and check the efficiency of the model [20].

$$Y = f(x_1, x_2, x_3 \ldots\ldots + x_n) \quad (1)$$

Where Y is the predicted response of the system, X_1 is the factors known as the variable of the action. The goal is to optimize the response variable (Y). It is assumed that the independent variables are continuous and controllable by experiments with negligible errors [20]. The true relationship between Y and Xn may be complex and unknown in most cases. However, in this case, by assuming low-order interactions may be estimated by factorial designs [22]. Individual second order effects cannot be estimated separately by 2n factor factorial designs. The first order model is as follows:

$$Y = b_0 + \sum_{i=1}^{k} \beta_i x_i + \sum \sum_{i<j}^{k} \beta_{ij} x_i x_j \quad (2)$$

Table 1: Experimental range and levels of independent variables for different stages of Nano – Chitosan Production and Phenol removal

Process Variable	-α	Low (-1)	Centre Point (0)	High (+1)	+ α
Demineralization					
A: Conc. of lactic acid (%)	4.95	7	10	13	15.05
B: Time (h)	0.32	1	2	3	3.68
C: Temperature (^{o}C)	36.59	40	45	50	53.41
Deproteination					

ISSN (online): 2645-2685; ISSN (print): 2756-6811

A: Conc. of NaOH (%)	0.64	2	4	6	7.36
B: Time (h)	1.32	2	3	4	4.68
C: Temperature(°C)	43.18	50	60	70	76.82
Deacetylation					
A: Conc. of NaOH (%)	9.77	20	35	50	60.23
B: Time (h)	1.32	2	3	4	4.68
C: Temperature(°C)	32.96	50	75	100	117.05
Nano – chitosan					
A: Conc. of STPP (%)	0.32	1	2	3	3.68
B: Time (h)	0.02	1	2.5	4	5.02
C: Conc. of Acetic Acid (%)	0.32	1	2	3	3.68
Phenol adsorption					
A: Adsorbent dosage (%)	1.32	2	3	4	4.68
C: Temperature (°C)	19.77	30	45	60	70.23
B: Time (mins)	-14.09	20	75	120	154.09

However, the CCD models, the positive values of β_{ij} indicates synergism of the effects of x_i *and* x_j while a negative value indicates antagonism between them. The number of runs required for the CCD comprises the standard, 2n factorial with its origin at center, 2n points fixed at a distance, α from the center to generate the quadratic terms, and replicate runs at the center, n is the number of the variables [20, 22]. The axial points are chosen such that they allow rotation. For three variables, the suggested number of runs is:

$$N = 2^n + 2n + nc = (2^3) + 2(3) + 6 \quad (3)$$

Where, N is total number of experimental runs, n is number of independent variables (factors) and nc is number of center points [21]. Once the desired ranges of values of the variables are defined, they are coded to at ±1 for the factorial points, 0 for the center points and ±α for the axial points. The codes are calculated as functions of the range of interest of each factor [22].

The mathematical relationship of the response Y with respect to the three independent variables x_1, x_2 and x_3 can be approximated by quadratic (second degree) polynomial Equation (4) as shown below:

$$Y = \beta_0 + \beta_1 x_1 + \beta_2 x_2 + \beta_3 x_3 + \beta_{12} x_1 x_2 + \beta_{13} x_1 x_3 + \beta_{23} x_2 x_3 + \beta_{11} x_1^2 + \beta_{22} x_2^2 + \beta_{33} x_3^2 + \cdots \quad (4)$$

Where Y is the predicted response, β_0 model constant; x_1,x_2 and x_3 are independent variables; β_1, β_2 and $\beta_3$are linear coefficients; β_{12}, β_{13} and β_4 are cross product coefficients and β_{11}, $\beta_{22}$and β_{33} are the quadratic coefficients [20]. The statistical significance of each regression coefficient for the various stages were determined by analysis of variance (ANOVA).

2.3 Demineralization of the Waste White Shrimp Shell

A modified procedure reported by [13] was used to carry out demineralization. About 2 g of prepared waste white shrimp shell sample was used in the ratio 1:5 (w/v) at specific conditions of lactic acid, temperatures and time as shown in Table1. Subsequently, equation (5) was applied to compute percentage degree of demineralization [14, 17] and optimal conditions shown in the Table 2.

$$DD_m = \frac{(A_o O - A_r R)x100}{A_o} \quad (5)$$

Where, DD_m is the Percentage degree demineralization (%), A_o is the Ash content before demineralization (%), A_r is the Ash content after demineralization (%), O is the Weight of Sample before demineralization (g) and R is the Weight of Sample after demineralization (g).

2.4 Nano-Chitosan Synthesis

About 5 g of milled Chitosan were primed in accordance to the specifications in Table 1. The formed nano-chitosan was washed several times with distilled water, filtered and oven dried at 60°C for 6 h [2, 10]. The average of particle size distribution was computed with the help of Dynamic light scattering (DLS). The efficiency of nano – chitosan was calculated using equation (6) and optimal conditions shown in the Table 2.

$$E = \frac{(M_o - M_t)x100}{M_o} \quad (6)$$

Where, M_o is the Weight of chitosan (g), Mt is the Weight of nano-chitosan (g) and E is the Efficiency (%).

2.5 Batch Adsorption

Batch adsorption was carried out using different conditions of some selected process parameters, namely, adsorbent dosage, contact time and temperature as shown in Table 1. The adsorbent (nano-chitosan) and Adsorbate (wastewater containing phenol), were mixed with aid of oscillating shaker. The mixture was subsequently separated with aid of centrifuge at 4000 rpm for 30 min and the collected supernatant solution was measured by double beam UV

spectrophotometer and compared with initial phenol concentration [2, 3]. The amount of phenol removed from Refinery wastewater (RWW) by the nano – Chitosan was calculated using equation (7) and optimal conditions shown in the Table 2.

$$R_e = \frac{(C_o - C_t)x100}{C_o} \quad (7)$$

Where, R_e is the percentage removal (%), C_o is the initial concentration (mg/l) and C_t is the final concentration (mg/l).

2.6 Characterization of Chitin, Chitosan and Nano-Chitosan

The surface functional groups of the shrimp shells, chitin, chitosan and nano-chitosan were determined by Fourier Transform Infrared (FTIR) spectroscopy. The data obtained were plotted with the aid of essential Fourier Transform Infrared (eFTIR) software [7, 11]. The surface morphology of the produced Chitosan and Nano-chitosan were obtained with aid of high-resolution Scanning electron microscopy (SEM) MEL-30000 – SCOTECH [14, 21]. The average of particle size of nano-chitosan distribution was obtained with the aid of Dynamic Light Scattering (DLS) – Malvern.

3. RESULTS AND DISCUSSION

3.1 Demineralization Process

The demineralization was carried out using experimental design matrix of central composite design (CCD) where the three selected process variables (concentration of acid, contact time and reaction temperature). The interaction between selected variables and their respective responses known as percentage degree of demineralization (%DDm) with validated model values were presented in Table 2.

The results of interaction between factors and response obtained from Table 2 shows that the factors of 9.76 % lactic acid concentration, 3 h and 50°C gives validated values of 99.57 and 99.62 % for experimental and predicted values respectively. The concentration of mineral composition, contribute to the total ash content value [24]. Each sample of demineralized WWSS were subjected to ash content test. The ash content values of each demineralized samples of 0.65 % were within the less than 1 % of quality chitin as reported by [21, 30, 31].

Table 2: Model Validation of chitin, chitosan, nano – chitosan and phenol removal

Stages	**Factors**		**Responses (%)**	
			% Degree of Demineralization	
			Experimental (CT-S)	Predicted (CT-S)
Demineralization (Chitin)	A	9.76 (%)	99.57	99.62
	B	3 (h)		
	C	50 (°C)		
			% Degree of Deproteination	
Deproteination (Chitin)	A	6.0 (%)	96.23	96.23
	B	3.34 (h)		
	C	70 (°C)		
			% Degree of Deacetylation	
			Experimental (CTS-S)	Predicted (CTS-S)
Deacetylation (Chitosan)	A	50 (%)	91.20	91.08
	B	3.4 (h)		
	C	85 (°C)		
			% Size Reduction	
			Experimental	Predicted
Nano-Chitosan	A	2.93 (%)	97.86	98.63
	B	3.77 (h)		
	C	2.95 (%)		
			% Phenol Removal	
			Experimental	Predicted
Phenol Removal	A	3.86 (g)		
	B	59.20 (°C)	97.22	97.61
	C	98.00 (min)		

ISSN (online): 2645-2685; ISSN (print): 2756-6811

3.1.1 Regression model developed for demineralization process

The mathematical relationship between the responses (%DDm) and independent variables (A, B, C) was generated to fit a general quadratic polynomial model that was selected as the most appropriate equation to represent the experimental data and authenticated by statistical tools such as coefficient of determination (Root-squared), Fisher value (F-value) and probability (P-value) using response surface regression [21]. Response surface methodology (RSM) of central composite design (CCD) was used for the development of quadratic regression equations [20]. The resulting model equations of demineralized samples from WWSS for both coded and actual were given as Equations (8), for R1-CTs (%DDm).

Final Equation in Terms of Coded Factors:

$$\mathrm{R1-CTs} = 96.70 + 6.65\mathrm{A} + 3.68\mathrm{B} + 0.94\mathrm{C} - 1.27\mathrm{AB} + 0.15\mathrm{AC} - 0.067\mathrm{BC} - 3.71A^2 - 1.58B^2 + 0.42C^2 + \cdots \quad (8)$$

From the CCD design, equation (8) was generated regression model as the ultimate model resulting from statistical analysis in terms of coded and actual factors for percentage demineralization [11, 20]. And were required to calculate coefficients of the quadratic model equation and predicted percentage demineralization of demineralized sample (response). The observed positive interactions of the generated regression model found that the A, B, C, A^2, B^2, C^2 and AB, AC and BC, terms were of high and moderate significance in explaining the individual and collaborative effects, respectively.

3.1.2 Analysis of variance (ANOVA) for demineralization process

The selected models were based on the highest sequential order polynomials according to the sequential sum of squares [20]. The quality of the models fitted was evaluated through analysis of variance (ANOVA) and its statistical significance was controlled by *F*-test. The analysis of variance (ANOVA) for quadratic model of demineralized process as presented in Table 3.

Table 3: ANOVA for Response Surface Quadratic Model of demineralization

Factor	Sum of square	Df	Mean square	F- value	p-value
Model	1044.725	9	116.0806	11.22546	0.0004
A-Conc of Acid	603.8447	1	603.8447	58.39421	< 0.0001
B-Time	184.623	1	184.623	17.85379	0.0018
C-Temperature	12.11135	1	12.11135	1.171217	0.3046
AB	12.88513	1	12.88513	1.246044	0.2904
AC	0.179521	1	0.179521	0.01736	0.8978
BC	0.035716	1	0.035716	0.003454	0.9543
A^2	198.0522	1	198.0522	19.15245	0.0014
B^2	35.77668	1	35.77668	3.459749	0.0925
C^2	2.523713	1	2.523713	0.244053	0.6320
Residual	103.4083	10	10.34083	-	-

R^2= 90.99 %; Adeq Precision = 11.824; Std. Dev. = 3.22

These observed positive interactions were further confirmed and authenticated by the *F* statistics and *P* values from Table 3. It was found that the Model F-value of 11.23 implies the model is significant. The value of "Prob > F" less than 0.0500 indicate model terms are significant. In this case A, B, A2 are significant model terms. Values greater than 0.1000 indicate the model terms are not significant. The authenticity of the models was further ascertained by their Standard Deviation of 3.22, Root Squared 0.9099 which is 91 %, Mean 93.38, Adjusted R-Squared 0.8289, Correlation of Variance 3.44 % and Adeq Precision 11.824, "Adeq Precision" measures the signal to noise ratio. A ratio greater than 4 is desirable and ratio of 11.824 indicates an adequate signal. The high values of Root Squared which was close to unity indicate the goodness of fit and that the experimental values were close to the predicted values [9].

ISSN (online): 2645-2685; ISSN (print): 2756-6811

3.1.3 Graphical analysis of the model for demineralization process

The generated regression equations by the software were graphically represented by the three-dimensional response surface plots as shown in Figures 1 – 3. These plots were used to understand the interactions of the three independent variables and to detect the optimal level of each variable for maximal response (%DDm) of demineralized sample.

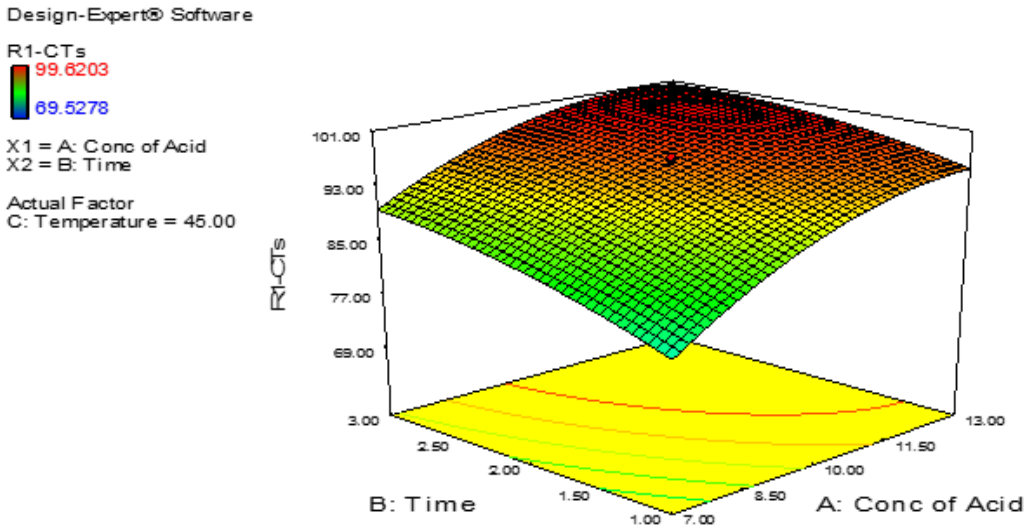

Figure 1: Combined Effect of Factors A-B on R1- CTs – demineralization

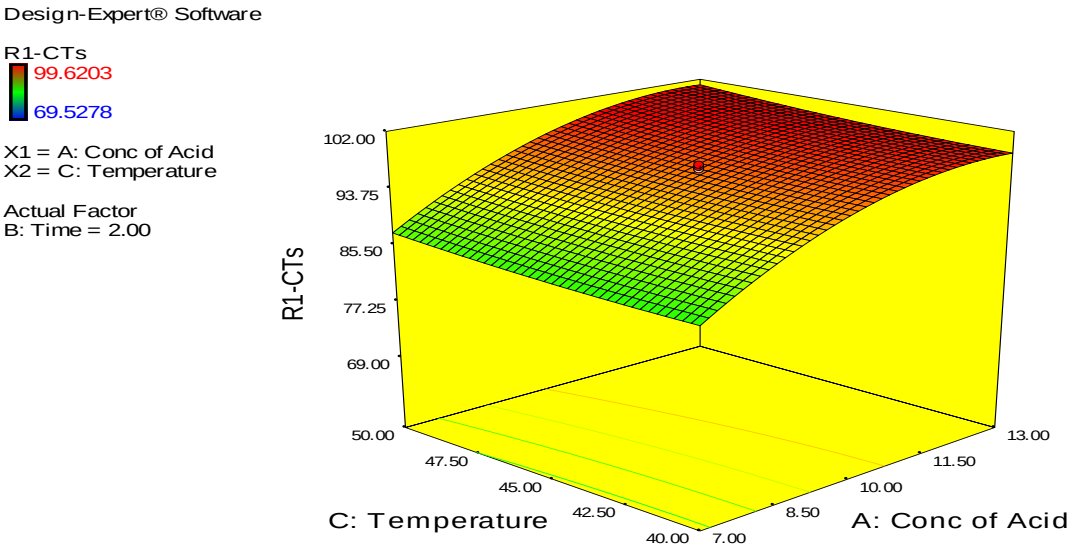

Figure 2: Combined Effect of Factors A-C on R1- CTs – demineralization

ISSN (online): 2645-2685; ISSN (print): 2756-6811

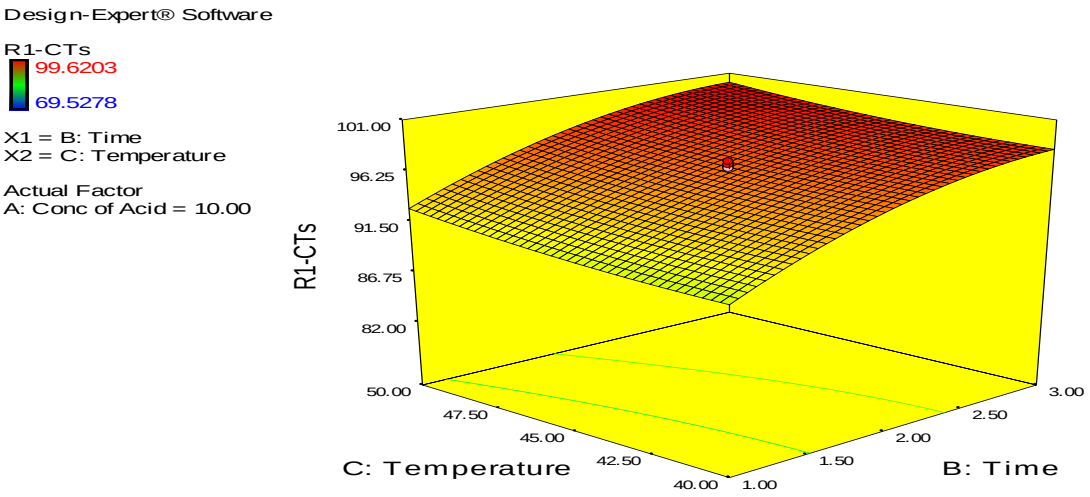

Figure 3: Combined Effect of Factors B-C on R1- CTs – demineralization

The plot represents the different combinations of two assessment variables simultaneously while maintaining zero level for the other variable [20, 21]. It can be observed that the removal efficiency (%) for mineral at each condition, the response range was 69.53 to 99.62 %. This indicates that the removal efficiency of mineral was a function of the studied contact time, temperature and concentration of lactic acid, which agrees with reported work of [9].

3.2 Deproteination Process

The deproteination was carried out with the aid of CCD through variation of three factors namely: concentration of Base, contact time and reaction temperature with optimal responses (percentage degree of deproteination – %DDp) as shown in Table 2. The resulted chitin was crushed to powdered form to facilitate deacetylation process. Also, the relationship between factors and response known as percentage deproteination (%DDp). The results of interaction revealed at factors of 6 % sodium hydroxide, 3.34 h and 70^{o}C gives model validated values of 96.23 % for both experimental and predicted values, which was closely above 96.0 % percentage deproteination reported by [31]. The crude protein content values of 13.56 % for chitin obtained was higher than 4.94 % protein content reported by [31]. This may be attributed to the location and the procedures applied during the preparation.

3.2.1 Regression model development for deproteination process

The percentage deproteinazed quadratic Model and highest order Sum of Squares suggested by the design of experiment. The resulting model equations for both coded and actual were given as (9).

Final Equation in Terms of Coded Factors:

$$\mathrm{Rp1-CTs} = 86.59 + 9.89\mathrm{A} + 8.02\mathrm{B} + 3.2\mathrm{C} + 5.03\mathrm{AB} - 1.83\mathrm{AC} + 0.25\mathrm{BC} - 4.67A^2 - 3.59B^2 + 0.95C^2 + \cdots \quad (9)$$

The percentage deproteination represented by generated regression models as the ultimate models resulting from statistical analyses in terms of coded and actual factors [11]. The observed positive interactions of the generated regression models were found to be A, B, C, A^2, B^2, C^2 and AB, AC and BC, coefficients were of high and moderate significance in explaining the individual and collaborative effects which were similar as reported by [32].

3.2.2. Analysis of variance for deproteination stage

The quality of the models fitted were evaluated through analysis of variance (ANOVA) and its statistical significance was controlled by *F*-test. The analysis of variance (ANOVA) for quadratic model of deproteinized stage are presented in Table 4.

It was seen from Table 4 that the Model F-value of 6.77 implies the model is significant. Values of "Prob > F" less than 0.0500 indicate model terms are significant. In this case A, B, A^2 are significant model terms. Also, validity of the models was further ascertained by Standard Deviattion of 7.06, Root Squared 0.8589 which is 86 %, Mean 80.30, Adjusted R-Squared 0.7320, Correlation of Variance 8.79 % , Predicted R-Squared -0.0316 and Adeq Precision 9.038, with a negative "Pred R-Squared" implies that the overall mean is a better predictor of the response (Rp1-CT$_s$,). A ratio greater than 4 is desirable and ratio of 9.038 indicates an adequate signal. The high values of Root Squared which was close to unity indicate the goodness of fit and the experimental values were close to the predicted values and closely agreed with reported work of [20].

ISSN (online): 2645-2685; ISSN (print): 2756-6811

Table 4: ANOVA for Response Surface Quadratic Model of deproteination

Factor	Sum of square	Df	Mean square	F- value	p-value
Model	3033.266	9	337.0295	6.765761	0.0031
A-Conc of NaOH	1335.844	1	1335.844	26.81664	0.0004
B-Time	878.7605	1	878.7605	17.64084	0.0018
C-Temperature	131.1141	1	131.1141	2.632074	0.1358
AB	202.7897	1	202.7897	4.070938	0.0713
AC	26.72902	1	26.72902	0.536576	0.4807
BC	0.515113	1	0.515113	0.010341	0.9210
A^2	314.4721	1	314.4721	6.312927	0.0308
B^2	185.9696	1	185.9696	3.733281	0.0821
C^2	12.9311	1	12.9311	0.259588	0.6215
Residual	498.1399	10	49.81399	-	-

R^2= 85.89%; Adeq Precision = 9.038; Std. Dev. = 7.06

3.3 Chitosan Synthesis (Deacetylation)

Since chitin generally, has low area of application due to the presence of strong hydrogen bond and inability to serve as good adsorbent [2], then the need to carry out deacetylation for the synthesis of chitin to obtained chitosan was very essential. The deacetylation which is the removal of acetyl group from chitin was carried out with the aid of CCD through variation of three factors namely: concentration of base, contact time and reaction temperature with their responses known as percentage degree of deacetylation (%DD) as shown in Table 2 [31].

However, the molecular weight of chitosan plays very important role in determining the possible industrial area of applications. Usually, the difference in the molecular weight is always attributed to the disparity in the degree of deacetylation in the formation of chitosan [33, 34], however, many other process parameters (factors) such as temperature, concentration of alkali, time, and procedure used in the synthesis of chitin could also influence the molecular weight of chitosan [24, 34,]. The results of interaction revealed at factors of 50 % sodium hydroxide, 3.4 h and 85^{o}C gives model validated values of 91.20 and 91.08 % for experimental and predicted values respectively, with molecular weight of 28336.84 Da. These values were higher than 60.69 % degree of deacetylation reported by [30].

3.3.1 Regression model development for deacetylation synthesis

The percentage degree of deacetylation quadratic Model and highest order Sum of Squares suggested by design of experiment software. The resulting model equations for both coded and actual were given as (10) [30].

Final Equation in Terms of Coded Factors:

$$\mathrm{R1-CTSs} = +85.99 + 2.82\mathrm{A} + 2.56\mathrm{B} + 3.38\mathrm{C} - 1.44\mathrm{AB} + 2.65\mathrm{AC} + 0.079\mathrm{BC} - 0.28A^2 - 0.75B^2 - 1.46C^2 + \cdots \quad (10)$$

From the CCD design, equation (10) was generated regression models resulting from statistical analysis in terms of coded and actual factors for percentage deacetylation [32]. The observed positive interactions of the generated regression model found that the A, B, C, A2, B2, C2 and AB, AC and BC, terms were of high and moderate significance in explaining the individual and collaborative effects.

3.3.2 Analysis of variance for deacetylation process

The quality of the models was evaluated through analysis of variance (ANOVA) and its statistical significance was controlled by *F*-test. The analysis of variance (ANOVA) for quadratic model of deacetylation process were presented in Table 5.

Table 5: ANOVA for Response Surface Quadratic Model of Deacetylation

Factor	Sum of square	Df	Mean square	F- value	p-value
Model	462.6889	9	51.40987	3.580153	0.0297
A-Conc of NaOH	108.3262	1	108.3262	7.543773	0.0206
B-Time	89.64149	1	89.64149	6.24258	0.0315
C-Temperature	155.8056	1	155.8056	10.85021	0.0081
AB	16.4935	1	16.4935	1.148598	0.3090

ISSN (online): 2645-2685; ISSN (print): 2756-6811

AC	56.00737	1	56.00737	3.90032	0.0765
BC	0.050124	1	0.050124	0.003491	0.9541
A^2	1.128402	1	1.128402	0.078581	0.7849
B^2	8.169367	1	8.169367	0.56891	0.4681
C^2	30.89989	1	30.89989	2.15185	0.1731
Residual	143.5969	10	14.35969	-	-

R^2 = 76.32 % , Adeq Precision = 6.536 Std. Dev. = 3.79

It was realised from Table 5 that the F-value of 3.58 implies the model is significant. Values of "Prob > F" of 0.0297 which is less than 0.0500 indicate model terms are significant. In this case A, B, C are significant model terms. The values that determine validity of the model are Standard Deviation of 3.79, Root Squared 0.7632 which is 76 %, Mean 84.28, Adjusted R-Squared 0.5500, Correlation of Variance 4.50 %, negative Predicted R-Squared of –0.7990 and Adeq Precision 6.536 implies that the overall mean is a better predictor of the response (R1-CTS). A ratio greater than 4 is desirable and ratio of 6.536 obtained indicates an adequate signal.

3.4 Nano-Chitosan Synthesis

The production of nano-chitosan was carried out with the aid of experimental design of central composite design (CCD). Three interacting factors were used such as concentration of STPP, concentration of acetic acid and contact time, as presented in Table 2.

Table 2 shows the design matrix consisting experimental runs of coded and actual factors with respect to responses as percentage size efficiency (R-NCTS). The resulted interaction shows that the factors of 2.93 % STTP, 3.77 h and 2.95 % Acetic acid gives model validation values of 97.86 and 98.63 % for experimental and predicted values respectively. It was observed from the experimental runs that an increase in concentration revealed higher particle size of nano chitosan (NCTS) and is gradually reduced with the lowering concentration. The nano chitosan size value at higher concentration may be due to the accumulation of polymer molecules and intermolecular cross linking through STPP spanning [35].

3.4.1 Regression model development of nano-chitosan synthesis

The percentage efficiency of nano – chitosan using quadratic Model and highest order Sum of Squares suggested that design of experiment show interaction of the parameters. The resulting model equations for both coded and actual were given as (11).

Final Equation in Terms of Coded Factors:

$$R1 = +82.30 + 12.51A + 10.82B + 5.12C - 4.12AB - 0.12AC + 1.88BC - 4.03A^2 - 5.26B^2 - 0.23C^2 + \ldots \quad (11)$$

From the CCD design, equation (11) was generated regression model as the ultimate model resulting from statistical analysis in terms of coded and actual factors for percentage size efficiency. The observed positive interactions of the generated regression model were found that the A, B, C, A2, B2, C2 and AB, AC and BC, terms were either high or moderate from the obtained responses.

3.4.2 Analysis of variance for nano-chitosan synthesis

The quality of the models fitted was evaluated through analysis of variance (ANOVA) and its statistical significance was controlled by *F*-test. The analysis of variance (ANOVA) for quadratic model of size efficiency were presented in the Table 6.

Table 6: ANOVA for Response Surface Quadratic Model of Nano-chitosan

Factor	Sum of square	Df	Mean square	F-Value	p-value
Model	4844.22	9	538.2462	5.334533	0.0076
A-Conc. of STPP	2138.82	1	2138.823	21.19777	0.0010
B-Time	1599.92	1	1599.915	15.85669	0.0026
C-conc. of Acetic Acid	357.62	1	357.6236	3.544391	0.0891
AB	136.13	1	136.125	1.349129	0.2724
AC	0.13	1	0.125	0.001239	0.9726
BC	28.13	1	28.125	0.278746	0.6090
A^2	233.62	1	233.6204	2.315401	0.1591
B^2	399.29	1	399.2895	3.957339	0.0747

ISSN (online): 2645-2685; ISSN (print): 2756-6811

C^2	0.73	1	0.733342	0.007268	0.9337
Residual	1008.98	10	100.8985	-	-

R^2= 82.76% Adeq Precision = 8.012 Std. Dev. = 10.04

These positive interactions values from Table 6 revealed that the Model F-value of 5.33 implies the model is significant. The values of "Prob > F" of 0.0076 which is less than 0.0500 indicate model terms are significant. In this case A, B, are significant model terms. The authenticity of the models was further ascertained by their Standard Deviation of 10.04, Root Squared 0.8276 which is 83 %, Mean 75.80, Adjusted R-Squared 0.6725, Correlation of Variance 13.22 % and Adeq Precision 8.012, "Adeq Precision" measures the signal to noise ratio. A ratio greater than 4 is desirable and ratio of 8.012 indicates an adequate signal.

3.4.3 Graphical model interaction for nano – chitosan

The generated regression equations by the software were graphically represented by the three-dimensional response surface plots as were shown in Figures 4 –6. These plots were used to understand the interactions of the three independent variables and to detect the optimal level of each variable for maximal response for percentage size efficiency of nano chitosan [20].

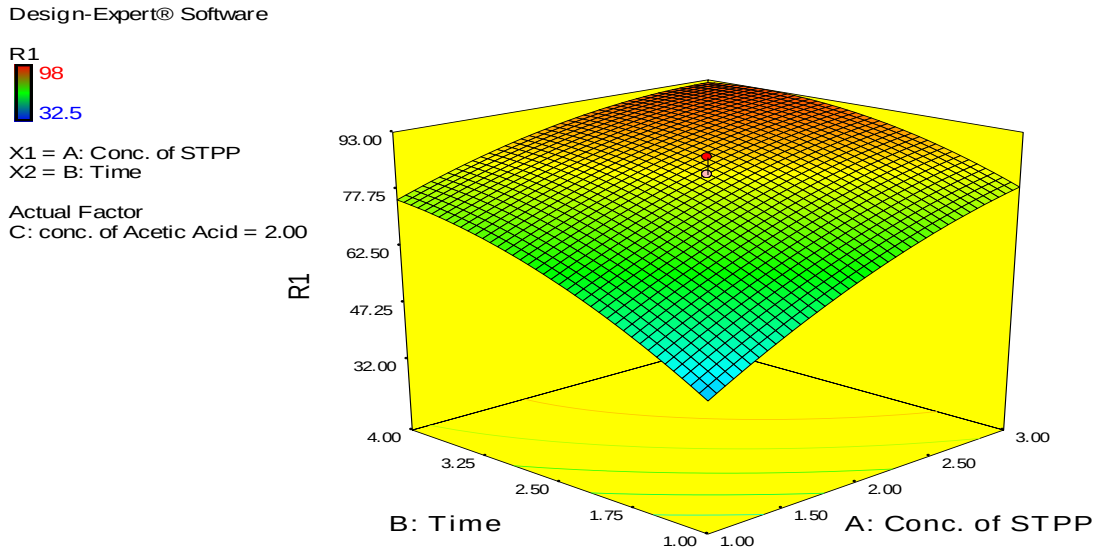

Figure 4: Combined Effect of Factors A-B on R1 – nano-chitosan

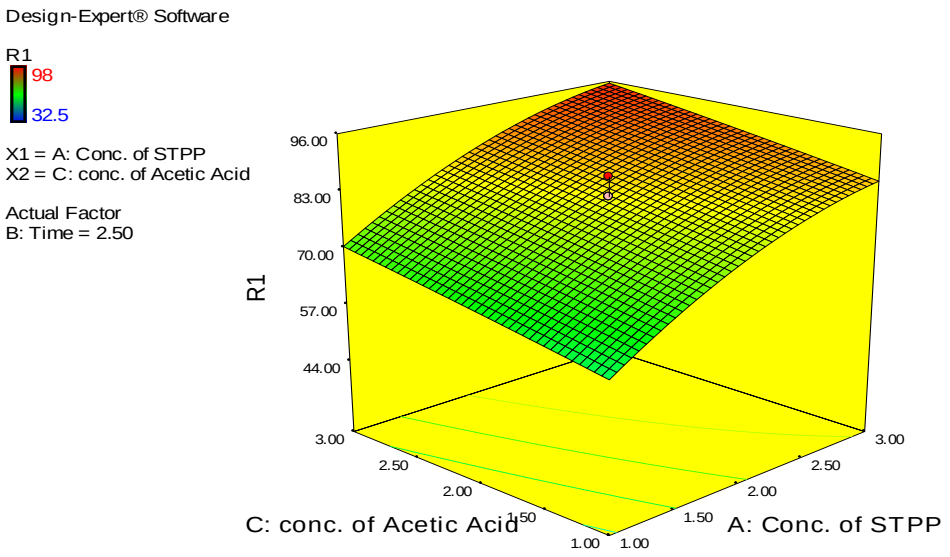

Figure 5: Combined Effect of Factors A-C on R1 – nano-chitosan

ISSN (online): 2645-2685; ISSN (print): 2756-6811

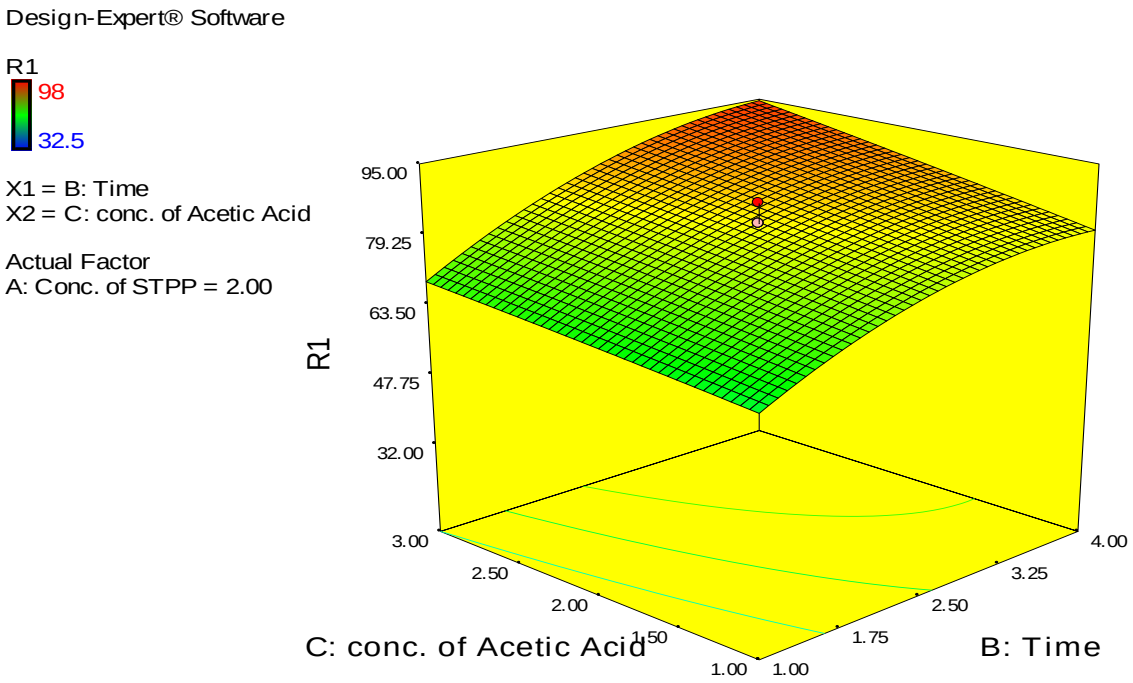

Figure 6: Combined Effect of Factors B-C on R1 – nano-chitosan

The response in terms of process variables was plotted in three-dimension as shows in Figure 4 shows the interaction of A and B revealed 98 % of percentage size efficiency at zero level of C. Figure 5 shows the interaction of A and C revealed 98 % of percentage size efficiency at zero level of B. Figure 6 shows the interaction of B and C revealed 98 % of percentage demineralization at zero level of A.

3.5 Phenol Adsorption Using Response Surface Methodology (RSM)

The limitations of this classical method can be effectively conquered by interactions of all the parameters collectively by statistical experimental designs such as Central Composite Design [20, 36]. Different process parameters such as adsorbent mass, contact time and temperature were taken as process variables for the experimental design with response as shown in the Table 1. The response was expressed as the percentage phenol removal (% R).

3.5.1 Regression model development for phenol removal

The resulting model equations of phenol removal for both coded and actual were given in Equations (12).
Final Equation in Terms of Coded Factors:

$$\mathrm{R-WK1} = +89.94 + 11.59\mathrm{A} + 4.28\mathrm{B} + 12.41\mathrm{C} - 0.51\mathrm{AB} + 1.38\mathrm{AC} - 0.35\mathrm{BC} - 6.05\,A^2 - 2.85B^2 - 7.52C^2 + \cdots \quad (12)$$

The CCD design, equations (16) generated regression model as the ultimate model resulting from statistical analysis in terms of coded and actual factors for percentage phenol removal [11, 37]. The observed interactions of the generated regression model found that the A, B, C, A2, B2, C2 and AB, AC and BC, terms were of high and moderate significance in explaining the individual and collaborative effects, respectively.

3.5.2 Analysis of variance for phenol removal process

The quality of the models was evaluated through analysis of variance (ANOVA) and its statistical tools such as coefficient of determination (Root-squared), Fisher value (F-value) and probability (P-value) as shown in the Table 7.

Table 7: ANOVA for Response Surface Quadratic Model of Phenol Removal (R – WK1)

Factor	Sum of square	Df	Mean square	F- value	p-value
Model	3033.266	9	607.55	6.60	0.0034
A-Adsorbent	1335.844	1	1834.31	19.94	0.0012
B-Temperature	878.7605	1	250.64	2.72	0.1298
C-Time	131.1141	1	2102.98	22.86	0.0007

ISSN (online): 2645-2685; ISSN (print): 2756-6811

AB	202.7897	1	2.08	0.023	0.8836
AC	26.72902	1	15.32	0.17	0.6918
BC	0.515113	1	0.97	0.010	0.9204
A^2	314.4721	1	527.03	5.73	0.0377
B^2	185.9696	1	116.75	1.27	0.2863
C^2	12.9311	1	814.06	8.85	0.0139
Residual	498.1399	10	92.01	-	-

R^2= 85.60%, Adeq Precision = 8.340 Std. Dev. = 9.59

Table 7 presents the Model F-value of 6.60 which implies the model is significant. The P – values of 0.0034 which is less than 0.0500 indicating model terms are significant. In this case A, C, A2, C2 are significant model terms. And the other values that determine validity of the model are Standard deviation of 9.59, Root Squared 0.8560 which is 86 %, Mean 78.73, Adjusted R-Squared 0.7263, Correlation of Variance 12.18 % and Adeq Precision of 8.340 indicates an adequate signal.

3.5.3 Graphical analysis of phenol removal process

The empirical predicted quadratic model for response (phenol removal, %) in terms of process variables was plotted in three-dimensional (3D) diagrams (Figure 7 – 9) to investigate the interaction among the variables for maximum removal efficiency of phenol from refinery wastewater.

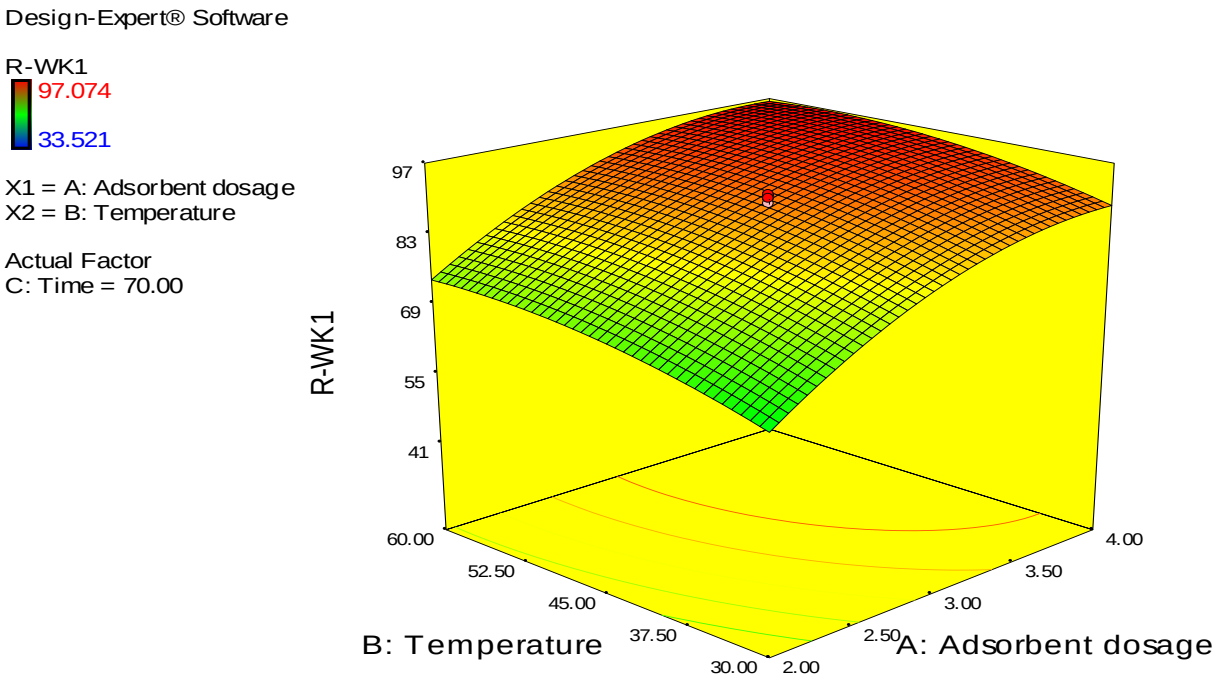

Figure 7: Combined Effect of Factors A-B on R-WK1

ISSN (online): 2645-2685; ISSN (print): 2756-6811

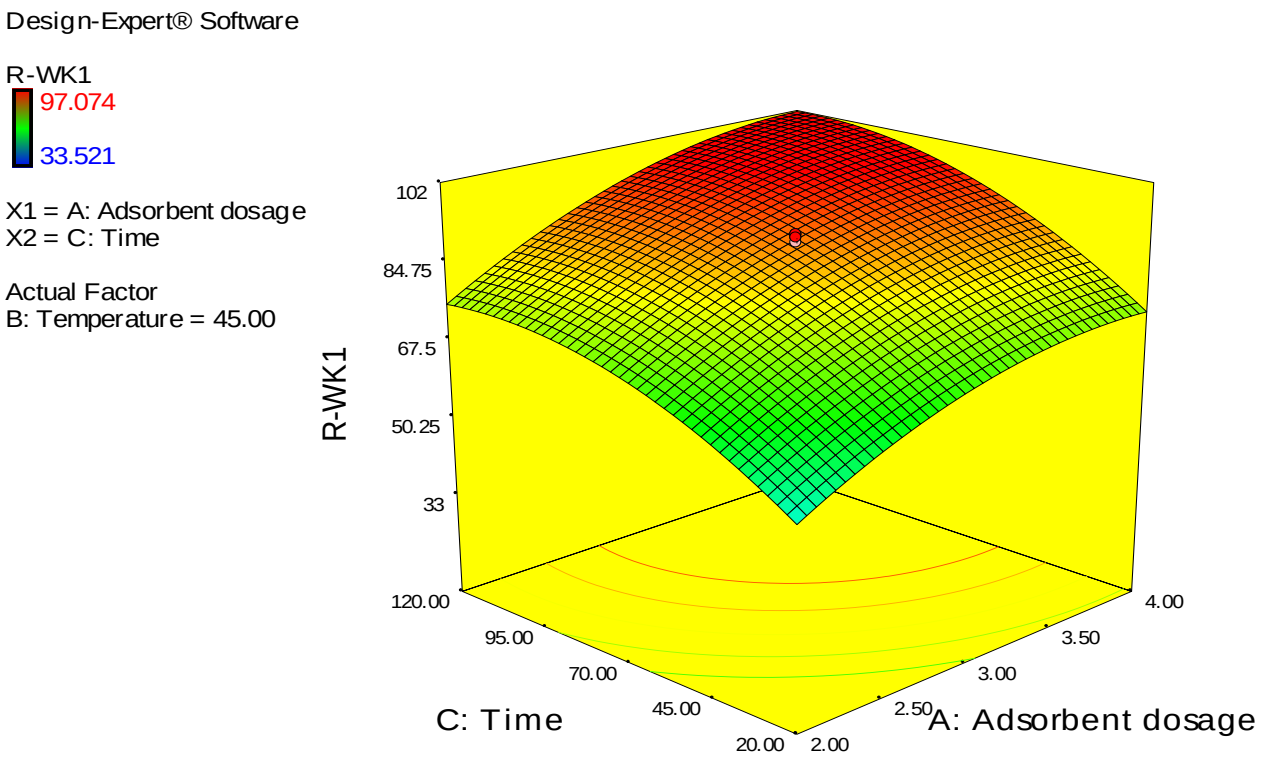

Figure 8: Combined Effect of Factors A-C on R-WK1

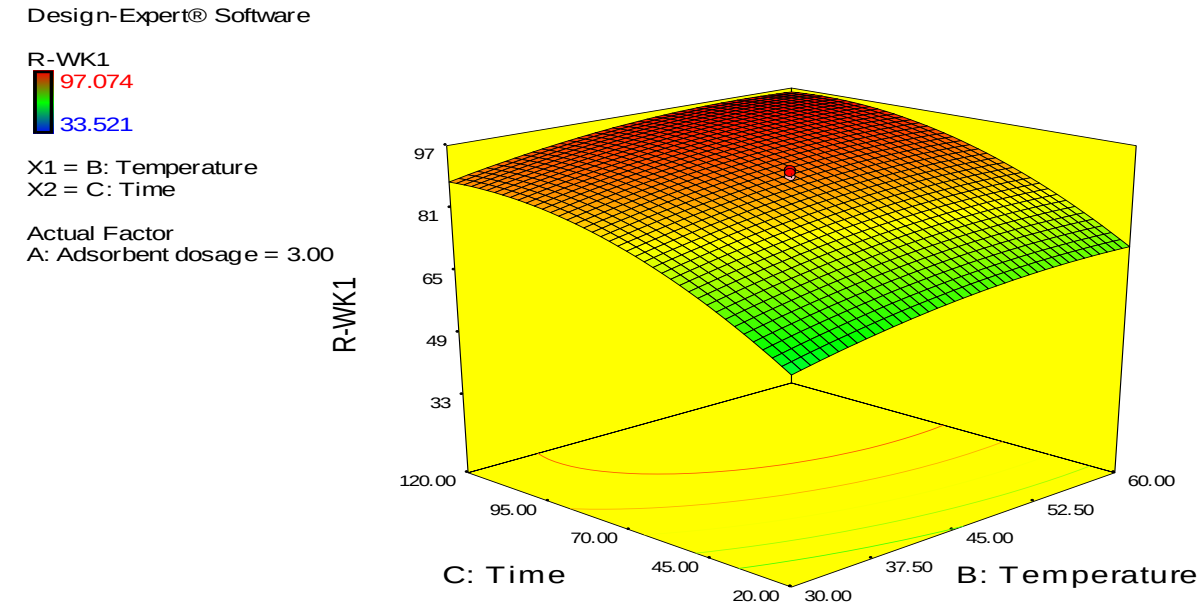

Figure 9: Combined Effect of Factors B-C on R-WK1

It can be observed that the removal efficiency (%) of the phenol at each condition, the response range was in range of 33.52 % to 97.07 %. This indicates that the size efficiency was a function of the contact time, temperature and adsorbent dosage.

ISSN (online): 2645-2685; ISSN (print): 2756-6811

3.6 Characterization of WWSS, Chitin, Chitosan and Nano-Chitosan

3.6.1 Proximate and surface chemistry of WWSS and Chitin

The proximate composition and surface analysis also known as Brunauer, Emmett and Teller – BET) of WWSS and the extracted chitin obtained were conducted. Analysis of the obtained results shows that WWSS and chitin contained 7.09 and 6.82 % moisture, 51.67 and 0.65 % ash content and 40.19 and 13.56 % crude protein respectively as shown in Table 8.

Table 8: Result of proximate and surface chemistry analysis of SSW and Chitin

Sample	Moisture (%)	Ash (%)	Lipid (%)	Crude Protein (%)	Crude fibre (%)	Surface Area (m^2/g)	Pore Volume (cm^3/g)
SSW	7.09	51.67	7.19	40.19	14.00	258.03	0.1606
Chitin	6.82	0.65	2.17	13.56	3.80	426.10	0.3714

The high ash content value observed in the WWSS is an indication that there is presence of mineral(s), which justified the need for demineralization. Consequently, the outcome of demineralization gives mineral removal as shown in Table 8. The resulted ash content of 0.65 % chitin was within the standard value of less than1as reported by [21]. The results of moisture, ash and protein content values obtained for WWSS and chitin in Table 8 were found to be similar to 8.27 and 4.30 % moisture, 46.01and 23.156 % ash and 65.763 and 0.870 % protein [39].

3.6.2 Fourier – transform infrared (FTIR) of the samples

The infrared spectra of WWSS, chitin, chitosan and nano – chitosan were presented in Figure 10. The broad and weak absorption bands noticed from 3600 $cm^{-1}$to 3000 cm^{-1} were due to the combined effect of NH and OH groups. The absorption band 3267cm^{-1}in chitosan (CTS-S) sample could be attributed to the N H secondary amine stretch.

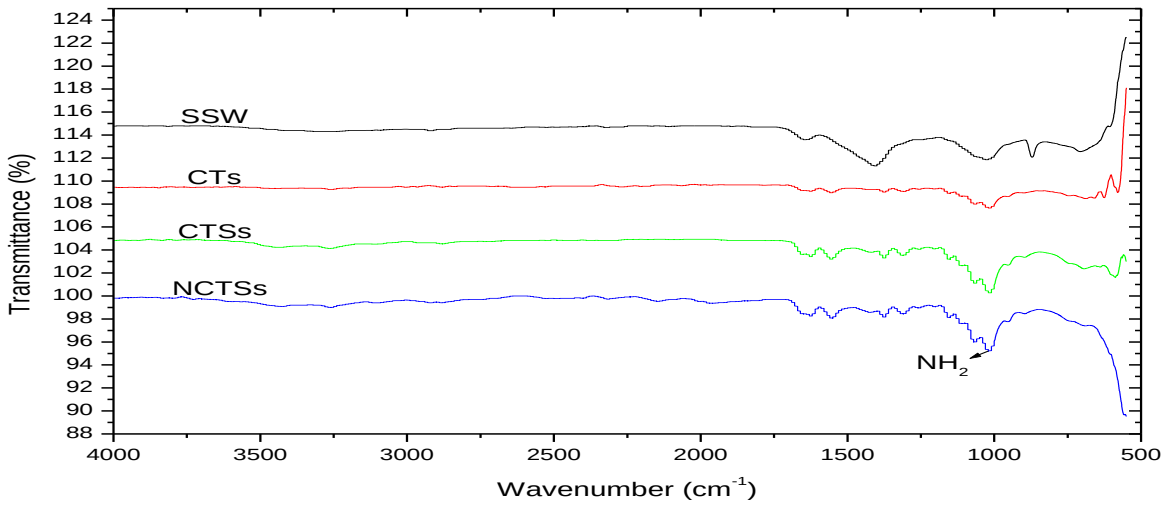

Figure 10: Infrared spectra of the shrimp (SS), chitin (CT-S), chitosan (CTS-S) and nano – chitosan (NCTS –S)

The weak absorption band in the region of 2750 – 2700 cm^{-1} was due to the presence of methylene and methyl groups in the chitin structure and originates due to the CH bond. The observed spectra also showed the presence of two bands in the region of 1647 – 1655 cm^{-1} for the samples of shrimp, chitin, chitosan and nano – chitosan respectively, which are due to the C O stretching vibration of the amide I bonds. The absorption peak at 1416$cm^{-1}$is due to the presence of NH of Amide II bond structure in the polymer. Bond absorptions in the region of 1410–700 $cm^{-1}$are due to a number of chemical functionalities in the saccharides ring such as OH. The FTIR spectra of shrimp shell wastes, chitin, chitosan and nano – chitosan was similar to vibration patterns reported by [33, 16].

3.6.3 Scanning electron microscope (SEM) of the samples

The morphological studies of chitosan and nano-chitosan samples were carried out through Scanning Electron Microscopy (SEM) as shown in Figure 11 – 12.

ISSN (online): 2645-2685; ISSN (print): 2756-6811

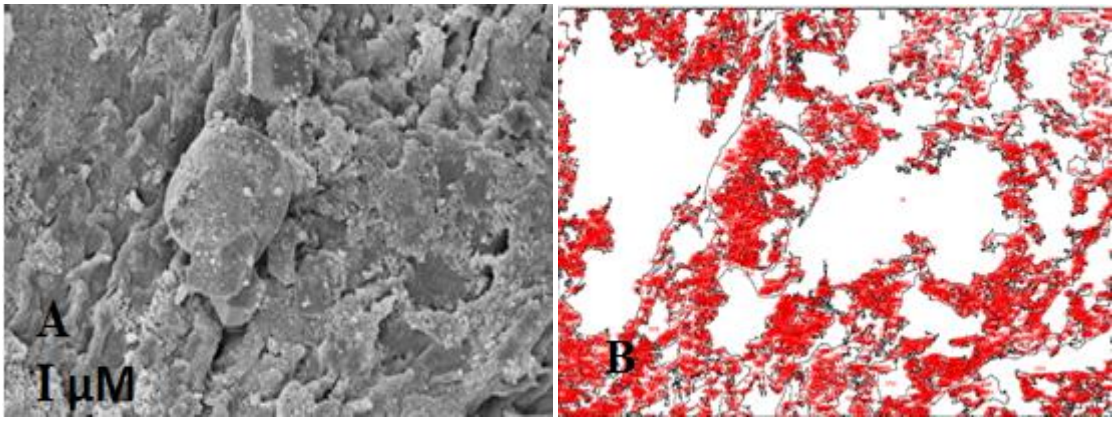

Figure 11: SEM Micrographs (A) and Image J (B) of Chitosan

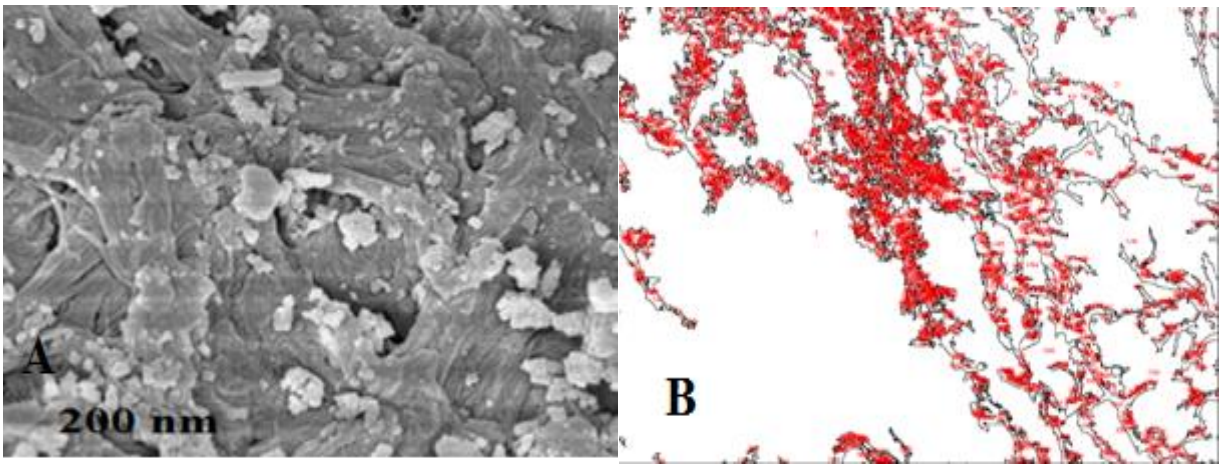

Figure 12: SEM Micrographs (A) and Image J (B) of nano – chitosan

The visual confirmation of the morphology and physical state of Chitosan and nano – chitosan surface were done via image J as shown in Figure 11 and 12 [43]. Image J software was used to describe the morphometric data and shape descriptions such as area, circularity, solidity, aspect ratio, and roundness as shown in Table 10[44].

Table 10: Morphormatric Shape and Statistic Data of the Chitosan and Nano –chitosan

	Area	**Circularity**	**Aspect Ratio**	**Roundness**	**Solidity**
CTSs					
Means	8.61 E-05	8.46 E-01	1.67 E+00	7.17 E-01	8.70 E-01
SD	3.15 E-03	2.49 E-01	8.00 E-01	2.71 E-01	1.74 E-01
Minimum	9.54 E-07	3.85 E-03	1.00 E+00	1.43 E-01	2.84 E-01
Maximum	1.83 E-01	1.00 E+00	7.02 E+00	1.00 E+00	1.00 E+00
NCTS					
Means	2.31 E-04	8.43 E-01	1.66 E+00	7.18 E-01	8.72 E-01
SD	5.71 E-03	2.50 E-01	8.00 E-01	2.67 E-01	1.65 E-01
Minimum	9.54 E-07	1.59 E-02	1.00 E+00	1.40 E-01	3.32 E-01
Maximum	2.53 E-01	1.00 E+00	7.17 E+00	1.00 E+00	1.00 E+00

It can be seen from Table 10 that the objective shape characteristics including circularity; indicate the degree of similarity to a perfect circle with designate value of 1.0 for a perfect circle. Solidity; describes the extent to which a shape is convex or concave [43, 44]. The solidity of a completely convex shape is 1, the farther the solidity deviates from 1, the greater the extent of concavity in the structure. Roundness; is similar to circularity but is insensitive to irregular.

4. CONCLUSION

The optimization of process parameters for the synthesis of nano–chitosan from white shrimp shell waste and subsequent use for phenol removal from refinery wastewater was achieved through RSM using CCD design matrix of experiments. The improved method of synthesizing chitin revealed the model validated for degree of demineralization and

deproteination were 99.57 %, and 96.23 % respectively. The degree of deacetylation and chitosan molecular weight were 91.20 % and 21374 Da respectively, which shows that the obtained chitosan was low molecular weight chitosan from WWSS. Spectroscopic techniques such as FT-IR and SEM are suitable for differentiating the structure of chitin, chitosan and nano–chitosan and revealed sites for phenol. The size of adsorbent (nano –chitosan) obtained was 84.36 nm from Dynamic Light Scattering (DLS), which create more surface area to facilitate adsorption process. The size efficiency of adsorbent at model validation was 97.86 % at 2.93 % concentration of STPP, 3.77 h and 2.95 % of acetic acid. The surface area of the adsorbent improves the removal efficiency of phenol as proved by RSM. For this study the model validation for phenol removal was 97.22 % at factors of 3.86 g, 59.20^{o}C and 98mins.

ACKNOWLEDGMENT

The authors would like to thank the Petroleum Technology Development Fund (PTDF) in Nigeria for the financial support.

REFERENCES

[1] Abdelkareem, M. (2013). Adsorption of Phenol from Industrial Wastewater Using Olive Mill Waste, *APCBEE Procedia*, 2013, paper 5, 349-357.

[2] Seyedi, S. M. Anvaripour, B. Motavassel, M. & Jadidi, N. (2013). "Comparative cadmium adsorption from water by nanochitosan and chitosan", *International Journal of Engineering and Innovative Technology*, 2 (9), 145-148.

[3] Farajzadeh, M. A. & Mohammad, R. F. (2005). Study of phenolic compounds removal from aqueous solution by polymeric sorbent, *Journal of the Chinese Chemical Society*, 52, 295-301.

[4] Amuda, O. S. Amoo, I. A. & Ajayi, O. O. (2006). Performance optimisation of coagulation/flocculation process in the treatment of beverage industrial wastewater, *Journal of Hazardous Materials*, 129, 69 – 72.

[5] Galambos, I. I. Molina, J. M. Jaray, P. Vatai, G. & Bekassy–Molnar, E. (2004). High organic content industrial wastewater treatment by membrane filtration. *Desalination*, 162, 117-120.

[6] Soto, M. L. Moure, A. Dominguez, H. & Parajo, J. C. (2011). Recovery, concentration and purification of phenolic compounds by adsorption: A review. *Journal of Food Engineering*, 25, 1–27.

[7] Krishnaveni, B. & Ragunathan, R. (2015). Extraction and Characterization of Chitin and Chitosan from solani F. CBNR BKRR, Synthesis of their Bionanocomposites and Study of their Productive Application. *Journal of Pharmaceutical Science & Research*, 7(4), 197-205.

[8] Peres, J. A. Beltran de Heredia, J. & Dominguez, J. R. (2004). Integrated Fenton's reagent - coagulation/flocculation process for the treatment of cork processing wastewaters. *Journal of Hazardous Materials*, 107, 115-121.

[9] Ravikumar, K. Pakshirajan, K. Swaminathan, T. & Balu, K. (2005). "Optimization of batch process parameters using response surface methodology for dye removal by a novel adsorbent," *Chemical Engineering Journal*, 25 (3), 15–138.

[10] Phawinee, N. Kittiwut, K. & Wanwisa, S. (2018). Isotherm and kinetic modeling on superparamagnetic nanoparticles adsorption of polysaccharide. *Journal of Environmental Chemical Engineering*, 6, (335 – 443).

[11] Ibrahim A. A., Abdulfatai J., Manase A., Muibat D. Y. (2017). Optimization and Modeling of Chitin Synthesis from Fish Scale Using Response Surface Methodology (RSM). *2nd International Engineering Conference (IEC 2017), Federal University of Technology, Minna, Nigeria, 2017*, 254 – 261.

[12] Muhammed, T. I. Alewo, O. A. Joseph, O. G. & Kenneth, K. A. (2012). Extraction and Characterization of Chitin from Nigerian Sources, *Leonardo Electronic Journal of Practices and Technologies*, 21 (3), 73-81.

[13] Islem, Y. & Marguerite, R. (2015). Chitin and Chitosan Preparation from Marine Sources. Structure, Properties and Applications, *marine drugs*, 13, 1133-1174.

[14] Hossain, M. S. & Iqbal, A. (2014). Production and characterization of chitosan from shrimp waste, *J. Bangladesh Argil. Univ.*, 12(1), 153–160.

[15] Anshar, P. (2013). Production and characterization of Chitosan from shrimp shells waste. *International Journal of the Bioflux Society*, 6 (4), 339 – 344.

[16] Pereira, A. G. Muniz, E. C. & Hsieh, Y. I. (2014). Chitosan-sheath and chitin-core nanowhiskers, *Carbohydrate Polymers*, 27, 158–166.

[17] Sawssen, H. Islem, Y. Olfa, G. Rachid, H. Marguerite, R. Kemel, J. (2014). Structural differences between chitin and chitosan extracted from three different marine sources, *International Journal of Biological Macromolecules*, 65, 298–306.

[18] Maram, T. H. A. Mohammed, R. & Maher, Z. E. (2013). Wastewater Treatment with Chitosan Nano Particles. *International Journal of Nanotechnology and Application*, 3, 39-50.

[19] Wijesena, R. N. Tissera, N. Kannangara, Y.Y. Lin, Y. Amaratunga, G. A. & De-Silva, K. M. (2015). A method for topdown preparation of chitosan nanoparticles and nanofibers, *Carbohydrate Polymers*, 117, 731–738.

[20] Atousa, G. K. & Narges, F. (2018). Treatment of textile dyeing factory wastewater by electrocoagulation with low sludge settling time: Optimization of operating parameters by RSM. *Journal of Environmental Chemical Engineering*, 6, 335 – 443.

[21] Abubakar, A. I. Abdulfatai, J. Muibat, D. Y. & Manase, A. (2017). Optimizing Deproteination of Chitin Using Response Surface Methodology, *1st National Conference on Chemical Technology, 2017*, www.narict.gov.ng/ncct.

[22]Bhaskar, N. Suresh, P.V. Sakhare, P. Z. & Sachindra, N. M. (2007). Shrimp biowaste fermentation with Pediococcusacidolactici CFR2182: optimization of fermentation conditions by response surface methodology and effect of optimized conditions on deproteination/ demineralization and carotenoids recovery, *Enzym. microb. Tech.* 40, 1427–1434.

[23] Ibrahim, A. A. Jimoh, A. Okafor, J. O. Abdulkareem, A. S. & Giwa, A. (2013). Effect of Lead Mining Activities on Crop Plants and Water: A Case Study of TungaTsauni, Gurara, Niger State, Nigeria, *International Journal of Engineering Research & Technology*, 2 (12), 755 – 765.

[24] Parthiban, F. Balasundari, S. Gopalakannan, A. Rathnakumar, K. & Felix, S. (2017). Comparison of the Quality of Chitin and Chitosan from Shrimp, Crab and Squilla Waste. *Current World Environment*, 12(3). Available from: http://www.cwejournal.org/?p=18529

[25] Chattopadhyay, D. P. & Inamdar, M. S. (2012). Studies on Synthesis, Characterization and Viscosity Behaviour of Nano Chitosan, *Research Journal of Engineering Sciences*, 1(4), 9-15.

[26] Rouquerol, J. Llewellyn, P. L. & Rouquerol, F. (2007). "Is the BET equation applicable to microporous adsorbents?", Characterization of porous solids VII, Studies in surface science and catalysis, *Elsevier*, 49–56.

[27] Gokoglu, N. & Yerlikaya, P. (2015). Chemical composition of fish in seafood chilling, refrigeration and freezing: science and technology, John Wiley and sons, Ltd, Chichester, Uk. Available: https://onlinelibrary.wiley.com.

[28] Klapiszewski, A. Wysokowski, M. Majchrzak, I. Szatkowski, T. Nowacka, M. & Jesionowski, T. (2013). Preparation and Characterization of Multifunctional Chitin/Lignin Materials, *Corporation Journal of Nanomaterials*, available: http://dx.doi.org/10.1155/2013/425726.

[29] Treeweranuwat, P. Boonyoung, P. Chareonpanich, M. & Nueangnoraj. K. (2020). Role of Nitrogen on the Porosity, Surface, and Electrochemical Characteristics of Activated Carbon. *American Chemical Society Omega*, 5, 1911−1918.

[30] Abdulwadud A., Muhammed, T. I., Surajudeen, A., Abubakar, J. M. & Alewo, O. A. (2013). Extraction and characterisation of chitin & chitosan from mussel shell, *Civil and Environmental Research*, 3(2), 248 – 262.

[31] Khorrami, M., Najafpour, G.D., Younesi, H. & Amini G.H. (2012). Growth kinetics and demineralization of shrimp shell using lactobacillus plantarum PTCC 1058 on Various Carbon Sources, *Iranica Journal of Energy & Environment*, 2(4), 320-325.

[32] Nouri, M. & Khodaiyan, F. (2015). Persian Gulf shrimp waste optimisation of chitosan extraction condition, *1st international conference on natural food hydrocolloids*, *Mashhad*, *Iran*, 2015, available: www.elsevier.com/locate/

[33] Ifuku, S. Nogi, M. Abe, K. Yoshioka, M. Morimoto, M. Saimoto, H. & Yano, H. (2009). Preparation of chitin nanofibers with a uniform width as alpha-chitin from crab shells. *Biomacromolecules*, 2(6), 1584–1588.

[34] Divya, K. Sharrel, R. & Jisha, M. S. (2014). A Simple and Effective Method for Extraction of High Purity Chitosan from Shrimp Shell Waste, *Proc. of the Intl. Conf. on Advances in Applied Science and Environmental Engineering*, *2014*,

[35] Dudhani, A. R. & Kosaraju, S. L. (2010). "Bioadhesive chitosan nanoparticles: Preparation and characterization", *Carbohydr. Polym.*, 81, 243-251.

[36] Zhou, Y. Ge, L. Fan N. & Xia, M. (2018). Adsorption of Congo red from aqueous solution onto shrimp shell powder, *Adsorption Science & Technology*, 36(5–6), 1310–1330.

[37] Manase, A. Mohammed, J. Philip, & B. L. T. Aboje, A. A. (2012). Preparation of activated carbon from oil palm fruit bunch for the adsorption of Acid Red 1 using optimized Response surface methodology, *International Journal of Engineering Research and Applications*, 2 (3) 1805-1815.

[38] Francesco, F. (2018). Optimization of a plant for treatment of industrial waste solutions: Experimental and process analysis. *Journal of Environmental Chemical Engineering*, 6, 377-385.

[39] Kaewboonruang, S. Phatrabuddha, N. Sawangwong, P. & Pitaksanurat, S. (2016). Comparative Studies on the Extraction of Chitin – Chitosan from Golden Apple Snail Shells at the Control Field. *Journal of Polymer and Textile Engineering*, 3 (1), 34-41.

[40] Dai, D.H. Wei-lian, H. Guang-rong, H. & Wei, L. (2011) Purification and characterization of a novel extracellular chitinase from thermophilic Bacillu ssp. Hu1, *Africa Journal of Biotechnology*, 10, 2476-2485.

[41] Agarry, S. E. & Aremu, M. O. (2012) Batch equilibrium and kinetic studies of simultaneous adsorption and biodegradation of phenol by pineapple peels immobilized Pseudomonas Aeruginosa NCIB 950. *British Biotechnology Journal*, 2(1), 26-48.

[42]Adejonwo O. A. (2016). Proximate and mineral Composition of Pseudotolithus senegalensisand Pseudotolithustypus from Lagos Lagoon, Nigeria, *Food and Applied Bioscience Journal*, 4(1), 35–40

[43] Gupta N, Rai A.L. (2013). Foramen ovale – morphometry and its surgical importance, *International Journal of Mental Health System*, 3, 4–6.

[44] Patil G.V, Shishirkumar, Apoorva D. (2014). Morphometry of the foramen ovale of sphenoid bone in human dry skulls in Kerala, *IJHSR*. 4, 90–93.